

# Effect of Gold Substrate on the Interface between Graphene Monolayer and an Ionic Liquid

Nicolas Gaudy, Mathieu Salanne,\* and Céline Merlet\*

Cite This: *ACS Nanosci. Au* 2025, 5, 84–92

Read Online

ACCESS |



Metrics &amp; More



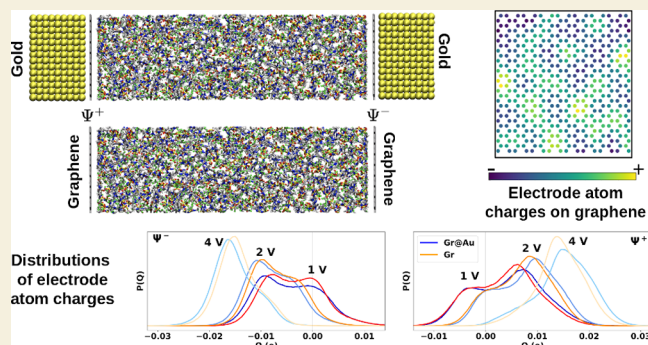
Article Recommendations



Supporting Information

**ABSTRACT:** The unique properties of graphene make it an ideal material for electrochemical studies, particularly of the electrochemical double-layer. However, experimental studies generally require depositing graphene on substrates like gold, that may affect the electronic structure of the electrode and thus the ions adsorption properties. This study explores the impact of gold substrates on graphene electrochemical behavior using molecular dynamics. Two systems were compared: graphene on gold (Gr@Au) and standalone graphene (Gr), with ionic liquid ([EMIM]-[TFSI]) as the electrolyte. The model accounts for the different metallic behavior of graphene and gold under the various applied potentials. Despite a similar electrolyte structure, the interfacial capacitance is affected, which can be attributed to different charge distributions within the electrode. The variations of the van der Waals and Coulomb energies also show some differences in the presence of gold, in particular for low potentials.

**KEYWORDS:** supercapacitors, molecular dynamics, EQCM, gold, graphene, ionic liquid, interface



## INTRODUCTION

Owing to its peculiar properties, graphene is widely investigated as an electrode material for various electrochemical applications.<sup>1</sup> In particular, its structure is simple and very stable. Unlike metals such as gold, there is no surface reconstruction under an applied potential, so that it is believed to be a perfect candidate for fundamental studies of the electrochemical double-layer (EDL). However, some difficulties arise when setting up the actual experiments. Indeed, it is difficult to perform measurements on freestanding graphene monolayers, so that they are generally deposited on a substrate.

For example, among the variety of experimental methods allowing to study the EDL, Electrochemical Quartz Crystal Microbalance (EQCM) stands as a powerful tool. It allows to investigate ion fluxes and redox reactions in electrochemical systems such as supercapacitors, batteries, and fuel cells.<sup>2–8</sup> In a nutshell, EQCM measures variations in the quartz crystal oscillations, related to the adsorbed mass on an electrode, for various applied potentials during an electrochemical experiment. To achieve this, the quartz crystal is sandwiched between two gold electrodes, allowing it to oscillate. It is then possible to deposit specific electrode materials on the gold to study the underlying energy storage mechanism.

EQCM is specially well adapted for nanoporous materials such as carbon or 2D materials such as graphene or MXene. For example, the deposition of a single layer of graphene on one side of the EQCM<sup>5,6</sup> enabled a dynamical study of

adsorption of ionic species on this surface. However, results are generally analyzed by accounting only for the deposited material, while the underlying gold layer could play an important role, in particular when nanometer thin materials are involved. Similar problems can arise when using other surface-specific spectroscopy or microscopy techniques. Such methods being increasingly used to investigate energy storage and conversion systems, it is thus important to study the influence of the substrate on the electrochemical response of the material and on the adsorption of ionic species on the surface. In previous works, we have studied the influence of the presence of a liquid on the adsorption properties of water nanodroplets<sup>9</sup> and on the adsorption of electrolytes within graphene nanopores.<sup>10</sup> Here we focus on the more difficult case of gold, which was chosen as a typical metallic substrate that may influence the EDL structure and properties.

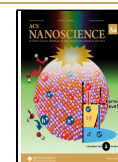
The presence of a gold substrate between the graphene layer can have two distinct effects on the interactions between the various atoms and molecules within the electrochemical double-layer. First, it displays a strong attractive interaction.

Received: November 22, 2024

Revised: January 22, 2025

Accepted: January 31, 2025

Published: February 7, 2025



This effect was put in evidence in classical molecular dynamics (MD) simulations, in which it was at the origin of the “freezing” of an ionic liquid electrolyte in direct contact with it.<sup>11,12</sup> In the simulations, this attraction is due to the Lennard-Jones parameters attributed to gold atoms, such as the ones provided by Heinz et al.,<sup>13,14</sup> that usually display a deep potential well. The latter is approximately 100 times larger than the one of carbon, which drastically modifies the interactions between the electrode and the electrolyte. Being short-ranged, this effect is expected to play a role only in the case of subnanometer thin deposited materials. Second, due to the contact between the two electronic conductors, an alignment of the Fermi levels accompanied by a charge transfer<sup>15,16</sup> should occur whose extent depends on a number of parameters, such as the type of adsorption of graphene on gold, the distance between layers, the applied potential,<sup>15</sup> etc. The presence of gold is therefore expected to alter not only the dynamics of the electrolyte but also the electronic structure of the material.

These two effects are therefore expected to play a particularly important role in the case where the investigated material is graphene. Indeed, it is possible to deposit monolayers of graphene on gold, which would result in the electrolyte being in the attractive region of the gold potential. In addition, graphene has a complex electronic structure near the Fermi level that can drastically be changed by the influence of gold. To study the influence of these effects, two systems were investigated and compared using MD simulations. The first system, designated as “Gr@Au”, consists in nine gold layers (111) covered with a graphene layer as electrodes, and the neat ionic liquid 1-ethyl-3-methylimidazolium bis-(trifluoromethylsulfonyl)imide ([EMIM][TFSI]) as electrolyte. The second system, designated as “Gr”, is the same but without the gold layers. A state-of-the-art approach, aiming at approximating the density of electronic states of the material depending on the applied potential,<sup>17</sup> is applied to represent the electrodes. We analyze the influence of gold on the capacitive behavior and dynamics of the system, and on the charge distribution on the electrodes. We also investigate the influence of energetics related to the gold electrode on the electrode/electrolyte interactions and on ion dynamics within the electrical double layer.

## METHODS

The MetalWalls software<sup>18,19</sup> was used to perform molecular dynamics (MD) simulations of neat [EMIM][TFSI] in contact with two graphene (Gr), or graphene/gold (Gr@Au), electrodes, between which a constant potential difference was maintained. The electrolyte comprises 326 ion pairs. The simulation boxes have respective dimensions of  $34 \times 37 \times 120$  and  $34 \times 37 \times 167$  Å<sup>3</sup>, with 2D periodic boundary conditions applied in the  $x$  and  $y$  directions—no periodic boundary conditions are applied in the  $z$  direction, perpendicular to the electrodes.<sup>20</sup> Typical snapshots of the two simulated systems are shown in Figure 1.

In the constant potential method, each electrode atom  $i$  carries a Gaussian charge distribution with a width  $\eta_i^{-1}$  and an amplitude  $Q_i$  given by

$$\rho_i(\mathbf{r}) = Q_i \eta_i^3 \pi^{-3/2} e^{-\eta_i^2 |\mathbf{r} - \mathbf{r}_i|^2} \quad (1)$$

where  $\mathbf{r} = (x, y, z)$  is the position considered in the simulation box and  $\mathbf{r}_i = (x_i, y_i, z_i)$  is the position of the  $i$ th electrode atom. The electrode atom charges fluctuate in order to satisfy the constant potential condition.<sup>20,21</sup>

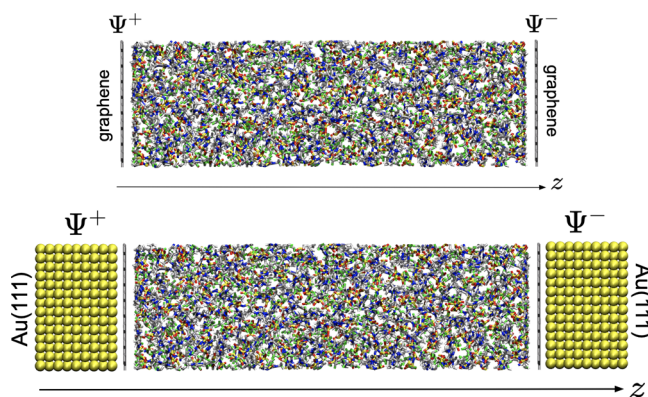


**Figure 1.** Supercapacitor composed of two graphene (Gr) electrodes at the top, or two graphene@gold (Gr@Au) electrodes at the bottom, in contact with a pure ionic liquid electrolyte [EMIM][TFSI]. Gray: graphene atoms, gold: yellow atoms.

In this work, the Gaussian width of the carbon atoms varies with the applied potential as a way to represent the peculiar density of states of graphene.<sup>17</sup> The Gaussian widths are given in Table 1. The

**Table 1. Parameter  $\eta^{-1}$  Used to Simulate Graphene Electrodes as a Function of Applied Potential  $\Delta\Psi$**

$\Delta\Psi$ (V)	0.0	0.2	0.5	1.0	2.0	4.0
$\eta_c^{-1}$ (Å)	0.04	0.1045	0.2395	0.4875	0.4	0.4

width of the Gaussian for gold atoms has been set in MetalWalls as  $\eta_{Au}^{-1} = 1.0591$  Å. This value is much larger than the one for graphene atoms whatever the potential; it reflects the highly metallic character of gold and has been chosen so that the capacitance is in agreement with the experimental data when modeling water in contact with gold electrodes.<sup>22</sup> In that case the Gaussian width is kept fixed with the applied potential. Each case was performed once for each condition.

On the electrolyte side, the charges carried by the atoms are considered to be point charges — note that no fluctuating charge model has been developed for ionic liquid electrolytes so far. Thus, the charge distribution of an atom  $i$  of charge  $Q_i$  is given by

$$\rho_i(\mathbf{r}) = Q_i \delta(\mathbf{r} - \mathbf{r}_i) \quad (2)$$

To represent [EMIM][TFSI], the all-atom CL&P force field<sup>23,24</sup> was employed. This force field includes intramolecular terms as well as electrostatic and van der Waals interactions. Atomic charges are scaled by a factor of 0.8 to mimic polarizability effects, a technique that has been suggested in previous studies of dense liquids.<sup>25–28</sup> The force field used for gold is the one developed by Heinz et al., which was widely used in previous studies,<sup>11,12,14,29–31</sup> while the one for the carbon atoms of the electrode is the one recently developed by Goloviznina et al.<sup>17</sup> A cutoff of 14.8 Å is used for van der Waals interactions, while the Ewald summation method is used to calculate long-range Coulombic interactions, with a real space cutoff of 17 Å. The initial configuration of the system was generated using the PACKMOL software.<sup>32</sup> The liquid density was adjusted by allowing the electrodes to move in the  $z$  direction, for a few nanoseconds, using a piston and applying a pressure of 0 bar on both sides of the system. Once the positions of the electrodes became stable, a bulk density of 1.6 g cm<sup>−3</sup> was attained, which is very close to the experimental value at ambient temperature for the studied ionic liquid.<sup>33</sup>

The simulations are conducted in the NVT ensemble using a time step of 2 fs. The temperature is set to 298 K using a Nosé–Hoover thermostat chain of length 5 with a relaxation time of 500 fs. A constant applied potential is maintained between the two electrodes.<sup>20</sup> Initially, an equilibration phase is performed at 0 V with a duration of 40 ns. Following this equilibration, a production run of 20 ns is carried out during which a constant nonzero potential is applied.

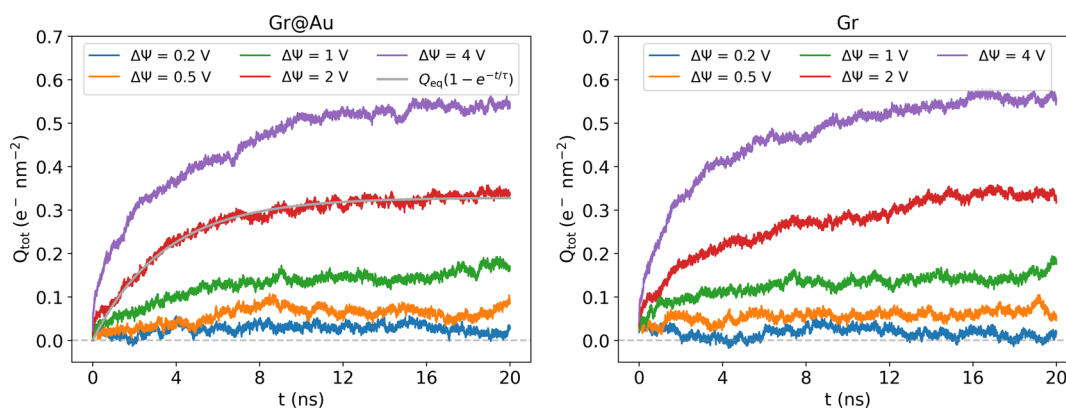


**Figure 2.** Total charge on the positive electrode,  $Q_{tot}$ , as a function of time for potential differences  $\Delta\Psi = 0.2, 0.5, 1, 2, 4$  V, for the gold/graphene electrodes (left panel) and the graphene electrodes (right panel).

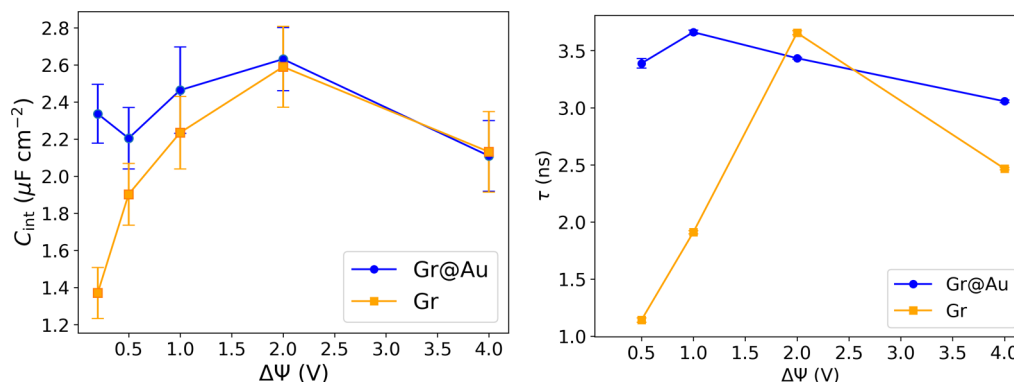


**Figure 3.** Integral capacitance (left panel) and characteristic charging time (right panel) as a function of the applied potential difference for the systems with and without gold.

## RESULTS AND DISCUSSION

### Effect of Gold Substrate on the Electrode Capacitance

After an initial equilibration at 0 V, a nonzero potential difference, between 0.2 and 4 V, is applied to the two systems. The time  $t = 0$  ns corresponds to the moment at which the potential is applied. Figure 2 represents the total charge carried by the positive electrode over time at different potentials. As expected, the larger the potential applied, the larger the charge building up on the electrodes. At first sight, the two systems behave in a similar fashion. However, the main differences are expected to occur at small potentials, when the graphene electrode has a smaller number of available electronic states. To better characterize and compare the charging process for the two systems and the various potentials applied, the curves were therefore fitted with an equation of the form  $Q_{eq}(1 - e^{-t/\tau})$  where  $Q_{eq}$  is the charge carried by the electrode at equilibrium and  $\tau$  is the characteristic time. The capacitance of the full capacitor was then calculated following  $C_{int} = Q_{eq}/\Delta\Psi$ .

The obtained results for  $C_{int}$  and  $\tau$  are plotted in Figure 3. The error bars associated with the capacitance values were calculated from the charge fluctuations around the mean value of the equilibrium charge  $Q_{eq}$  after the equilibrium is reached, and the error bars associated with the values of  $\tau$  are obtained from the covariance matrix of the fit. Due to a large uncertainty for the evaluation of  $\tau$  for the lowest applied potential (0.2 V), this point was omitted on the Figure. The capacitance in the presence of gold is larger than the capacitance of graphene alone which is consistent with previous work on graphite

electrodes,<sup>17</sup> in which it was shown that accounting for the density of states in the electrode model lead to a drastic decrease of the capacitance at low potentials, an effect which is generally accounted for within a so-called “quantum capacitance” term.<sup>34</sup> In the present work, this effect is accounted by adjusting the electrode charges Gaussian width as discussed in the Methods section. For higher applied potential differences, a decrease in capacitance is observed independently of the nature of the system. This is due to a phenomenon of overscreening that intensifies as the potential increases.<sup>35,36</sup>

Although it is not straightforward to compare the calculated capacitances with experimental values since the latter are generally reported for single electrode studies (while our integral capacitance accounts for the two EDLs capacitances, which are in series), we note that the order of magnitude is in good agreement with recent measurements by Yang et al.<sup>37</sup> They report values ranging between 1 and 5  $\mu\text{F cm}^{-2}$  for the positive electrode with a single layer of graphene deposited on a  $\text{SiO}_2$  substrate, which is consistent with our results with the standalone graphene electrode (typically  $C_{int}$  would have to be multiplied by two if the two double-layer have similar capacitances). This is coherent since  $\text{SiO}_2$  is not expected to have a similar effect as Au on the electronic structure of graphene, being an electronic insulator.

While the difference in capacitance could be due to modifications of the electrolyte structure, the charge distribution in the electrodes or a combination of both, Supplementary Figure S1 shows that there is no major



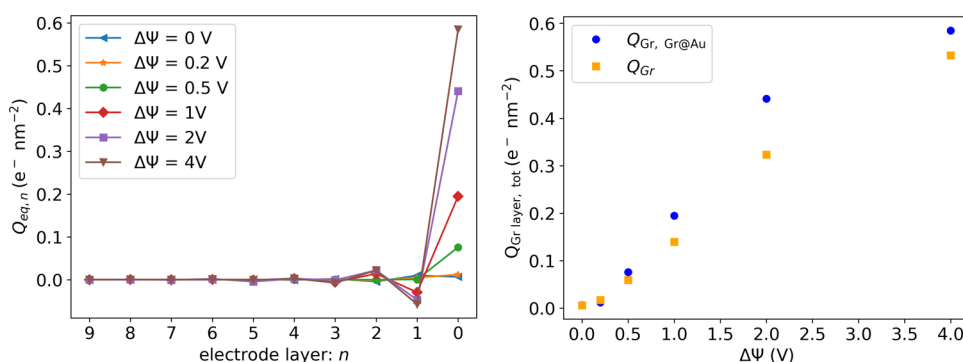


**Figure 4.** Left panel: Total charge carried by each of the  $n$  planes of atoms which form the Gr@Au electrode ( $n = 0$  corresponds to the graphene plane and  $n \geq 1$  the gold planes). Right panel: Average value of the total charge carried by the graphene electrode once the system has reached equilibrium,  $Q_{eq,Gr}$  as a function of the applied potential difference.

difference between the atomic densities between the systems with and without gold substrate. It thus seems that the difference is mostly due to the charge distribution in the electrodes and on the charge response properties as controlled by the underlying model.

Similar differences are also observed between the two systems concerning the characteristic charging times. It can be seen that the charging dynamics are, in the case of low potentials, slower in the presence of gold electrodes. This suggests that, indeed, the presence of gold has an influence on the dynamics of the electrolyte at the interface with the electrode which in the turn has an impact on the charging dynamics. Such a result is not surprising since for such planar interface the charging time is expected to scale as  $\tau \approx R C_{int}$  where  $R$  is the resistivity, that should barely change between the two systems. The variation in the characteristic time can therefore be attributed to the changes in capacitance due to the gold substrate.

#### Effect of Gold Substrate on the Charge Carried by Graphene

To investigate the charge distribution in the electrodes, we first analyze how the charge distributes between the graphene layer and the gold material. The left panel of Figure 4 shows the total charge carried by each electrode plane where  $n \in [1; 9]$  corresponds to the 9 gold planes index. The  $n = 9$  is the gold plane furthest away from the electrolyte,  $n = 1$  is the gold plane in contact with the graphene and  $n = 0$  is the graphene plane itself, in contact with the electrolyte. As expected, the graphene layer in contact with the electrolyte carries the largest excess charge, consistently with previous works.<sup>38</sup> Then, from one plane to the next, the excess charge sign alternates, in agreement with charge compensation processes. The excess charge, i.e. the amplitude of these oscillations, increases with the applied potential and decreases with the depth within the bulk of the electrode. This behavior is consistent with previously published works.<sup>39</sup>

The right panel of Figure 4 shows the total charge carried by the graphene layer with and without the presence of gold as a function of the potential difference. This outer surface charge is larger in the presence of gold, which is consistent with the increase of capacitance reported above. This effect can be attributed to the larger metallicity of the gold electrode as represented within our model.

Figure 5 shows the distribution of atomic charges carried by the graphene electrode with and without the presence of gold. We can see that there are differences in the distributions (i)

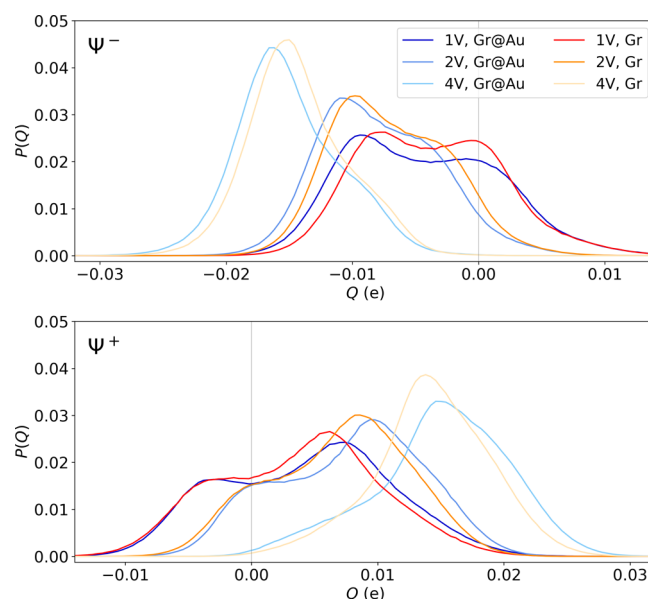


**Figure 5.** Distributions of atomic charges carried by the carbon atoms of the graphene electrodes, on both the negative (top panel) and positive (bottom panel) electrodes for the Gr@Au and Gr systems.

between the negative and positive electrodes, and (ii) between the systems with and without gold. The difference between the negative and positive electrodes is expected since the ions adsorbed are not the same depending on the polarity. On the negative electrode side, EMIM cations are present in majority while on the positive electrode TFSI anions dominate. The adsorption of ions locally modifies the charge response of the electrode, so the adsorption of TFSI or EMIM will not result in the same electrical response at the surface of the material. Such asymmetric behavior between negative and positive electrodes have already been observed in the literature.<sup>39,40</sup> Also, at low voltage, the charge distribution exhibits a double peak, which transitions to a single peak at higher voltage. The type of adsorbed ion locally alters the electrode response, making the composition of the first adsorption layer crucial to the observed atomic charge distribution. At higher potentials, this layer primarily consists of counterions, whereas at lower potentials, it includes a mix of counterions and co-ions (see Figure S2 in SI). This leads to a more diverse charge response at low potentials, with the double-peak distribution vanishing as the potential increases. We note that in a previous work on graphene-aqueous electrolyte using a QM/MD approach,

Elliott et al. also observed a nontrivial distribution of the electrostatic potential felt by the carbon atoms.<sup>41</sup>

Regarding the effect of gold, its presence modifies the interactions between the electrode and the electrolyte and also between the gold electrode and the graphene electrode. The effect of the modified interactions between electrode and electrolyte on the adsorbed electrolyte properties will be investigated in more details in a later section. In the presence of gold, the whole charge distributions are shifted toward larger values, for both the negatively and positively polarized graphene electrode compared to when gold is absent - note that a similar behavior is also observed for smaller applied potentials (shown for  $\Delta\Psi = 0.2$  and 0.5 V in SI). It is worth noting that the effect is more pronounced on the side of the distributions corresponding to the larger atomic charges.

### Effect of Gold Substrate on Charge–Charge Correlation Functions

In order to study the difference in the spatial correlation of the charges on the atoms of the graphene layer in the presence or absence of the gold layer, we calculated radial charge–charge correlation functions in the graphene layer following

$$C_s(r) = \frac{\langle (Q_i(\mathbf{r}_i) - \langle Q_{\text{tot}} \rangle)(Q_j(\mathbf{r}_j) - \langle Q_{\text{tot}} \rangle) \rangle}{\langle Q_{\text{tot}}^2 \rangle - \langle Q_{\text{tot}} \rangle^2} \quad (3)$$

where  $Q_i(\mathbf{r}_i)$  is the charge carried by the  $i$ th atom of the graphene electrode identified by the coordinates  $\mathbf{r}_i = (x_i, y_i)$  as shown in Figure 6. The distance between atoms  $i$  and  $j$  is  $r = |\mathbf{r}_i - \mathbf{r}_j|$ .

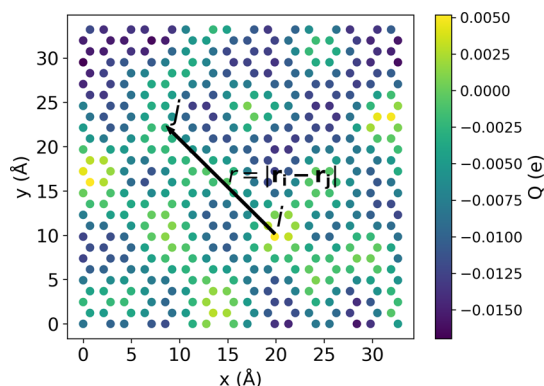


**Figure 6.** Visualization of the instantaneous charges, for a randomly chosen configuration, on the negatively polarized graphene electrode in the  $(x, y)$  plane. The color represents the charge carried by a carbon atom for an applied potential difference of  $\Delta\Psi = 2$  V. The definition of the distance between two electrode atoms, used in the calculation of charge–charge correlation functions, is illustrated.

–  $\mathbf{r}_j|$ . The symbol  $\langle \cdot \rangle$  represents an average over the configurations. This analysis is similar to the one conducted by Scalfi and Rotenberg.<sup>42</sup> Examples of charge–charge correlation functions at applied potential differences equal to 1, 2 and 4 V are shown in Figure S4.

According to the definition of the charge–charge correlation function, the closer it is to 1, the larger the correlation between the charges of the two atoms. On the other hand, the weaker the correlation between charges, the closer the correlation function will be to 0. For  $r = 0$ ,  $C_s(r) = 1$ , as this case corresponds to a single atom, which is completely correlated with itself. The larger the distance between the two atoms, the weaker the correlation, which tends toward 0 at large enough

distances. In order to extract a characteristic correlation length  $r_s$  between two charges on the graphene electrode, the correlation curves were fitted using the function

$$C_s^{\text{fit}}(r) = e^{-r/r_s} \cos(ar/r_s + b) \quad (4)$$

where  $a$ ,  $b$  and  $r_s$  are the parameters of the fit.

The characteristic correlation distances  $r_s$  obtained for the two systems as a function of the potential difference are shown in Figure 7. The correlation distance decreases as a function of

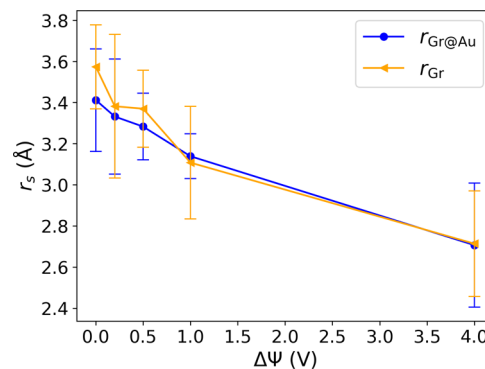


**Figure 7.** Characteristic charge–charge correlation distance  $r_s$  between charges of atoms present in the graphene electrode in the presence or absence of gold, as a function of the applied potential difference.

the potential difference. There is no major difference between the two systems. As the width of the graphene Gaussian was adapted as a function of the applied potential, this amounts to modulate the charge density in the material. The higher the potential difference, the more charge carriers are introduced into the material, increasing the electrostatic screening and leading to a reduction in the length of the charge–charge correlation. An identical effect was observed in the work of Scalfi et al.<sup>42</sup> when the Thomas-Fermi length is modulated.

Graphene is arranged in a hexagonal lattice, where the shortest distance between two atoms is 1.42 Å,<sup>43</sup> and the longest is 2.84 Å. At low potentials, close to 0 V, charge–charge correlations extend beyond a single hexagon. However, at a potential difference of 4 V, the charge correlations are contained within a hexagon.

### Effect of Gold on the Interaction Energy between Electrolyte and Electrode

We have seen that the presence of gold mostly affects the charge distribution in the electrode and charging dynamics. In this section, we investigate how the interaction energies between the adsorbed electrolyte atoms and the electrode atoms are affected by the presence of gold. The atoms are considered adsorbed if they are at a distance below 6.6 Å from the electrode, corresponding to the first minimum of the atomic density (see Figure S1). At each time step, the Coulomb and Lennard-Jones interaction energies of all the atoms in the double layer and all the atoms in the electrode are calculated. It should be noted that the cut-offs defined in MetalWalls to calculate those energies were also applied here. The results presented in this section are the mean value of these energies once the system is charged for an applied potential difference of  $\Delta\Psi = 1$  V.

The left panel of Figure 8 shows the average electrostatic interaction energy between the atoms of the ions in the first

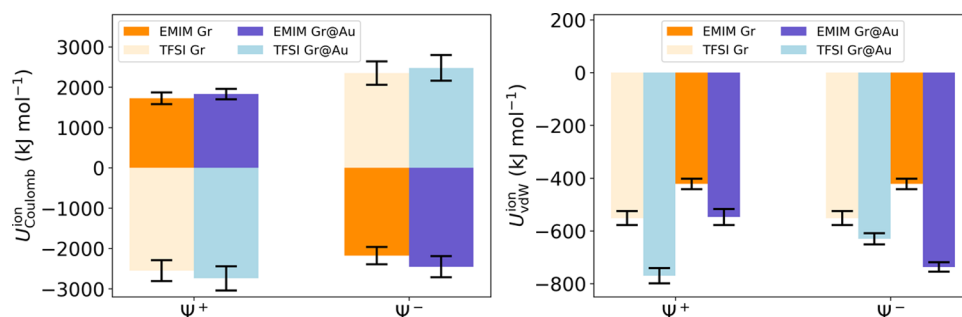


**Figure 8.** Average electrostatic energy (left) and van der Waals energy (right) between adsorbed electrolyte atoms and electrode atoms for a potential difference of 1 V.

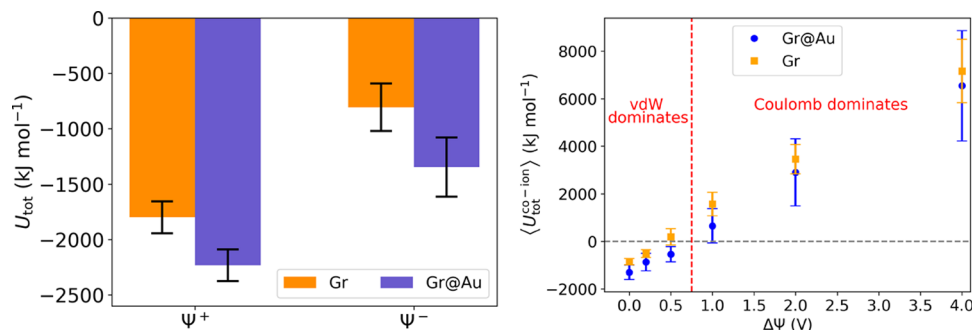


**Figure 9.** Left: Average total interaction energy between the adsorbed electrolyte atoms and the electrode, on the negative and positive electrode sides, for a potential difference of 1 V. Right: Average total energy of the co-ions as a function of applied potential difference such as  $\langle U_{\text{tot}}^{\text{co-ion}} \rangle = \langle U_{\text{vdW}}^{\text{co-ion}} \rangle + \langle U_{\text{Coulomb}}^{\text{co-ion}} \rangle$ . The average van der Waals energy of the co-ions being strictly negative, and the average Coulomb energy of the co-ions being strictly positive, the sign of the total energy indicates which of the two energies is predominant.

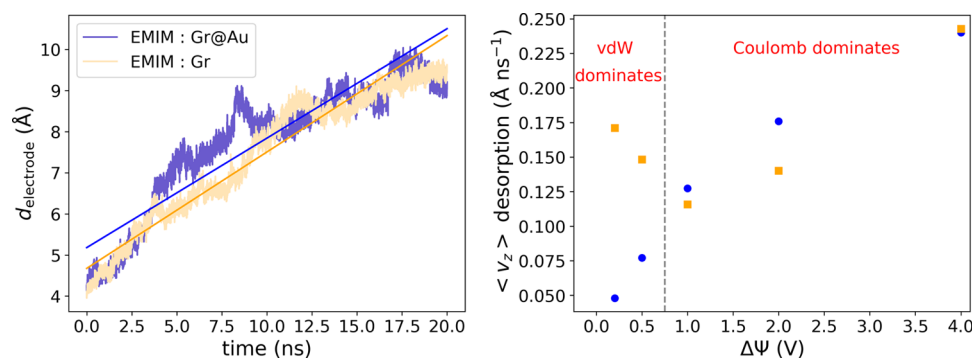


**Figure 10.** Left: Average distance to the positive electrode of the co-ions, as a function of time for a potential difference of  $\Delta\Psi = 4$  V. Right: Average co-ion desorption velocity in the presence and absence of gold as a function of the applied potential.

adsorbed layer and the atoms of the electrode. The results show that the counterions minimize the electrostatic interaction energy while the co-ions maximize it. In absolute terms, the amplitude of the interaction energy between the TFSl anions and the electrode atoms is larger than for the EMIM cations. Finally, there is no major difference between the systems with and without gold electrodes. It thus seems that the difference in charge distributions does not affect significantly the electrostatic interactions.

The right panel of Figure 8 shows the average van der Waals interaction energy between the ions in the first adsorbed layer and the electrode atoms of the electrode. In this case, there is a difference between the systems with and without gold. The presence of gold increases the contribution of van der Waals energy to the interaction between the atoms of the first adsorbed layer and the electrode. Although this interaction is short-range and the gold electrode is located behind the

graphene layer, the presence of gold increases the attraction of the ions toward the electrode.

Figure 9 (left panel) shows the average total interaction energy between adsorbed atoms and electrode atoms. The interaction energy is larger on the positive electrode side than on the negative electrode side. As seen on Figure 8, this is due to a higher concentration of TFSl on the positive electrode side, which have a higher interaction energy with the electrode atoms. The evolution of the total interaction energy with applied potential difference is shown in Figure 9 (right panel). At low potentials, the Coulomb energy is small compared with the van der Waals energy, which then dominates the interactions between the electrolyte and the electrode. On the other hand, as the applied potential increases, the Coulomb energy dominates the interactions in the system.

## Effect of Gold on Ion Dynamics at the Interface

We now try to correlate the dynamics of ions in the first adsorbed layer with energies. In particular, we are interested in the ions desorbing during electrode charging. In order to determine an average desorption velocity, we identify all the co-ions desorbing and calculate their average distance to the electrode over time. Figure 10 (left panel) shows the results for EMIM cations desorbing during charging of the positive electrode with and without gold. Using a linear regression, we extracted the slope of this function which gives us the desorption velocity. Once the slope has been extracted, the velocity obtained for the EMIM and TFSI of each system is averaged. We expect that stronger attractive interactions between electrolyte atoms and the electrode will lead to slower dynamics.

Desorption velocities obtained for all applied potential differences are shown in Figure 10. At low potentials, we observe a clear qualitative and quantitative difference in ion dynamics between the system with and without gold. As was seen in Figure 9, for these potentials, the van der Waals energy dominates over the Coulomb energy. The presence of gold increases the van der Waals interactions between the electrode and the electrolyte, slowing down the dynamics of the ions. For higher applied potentials, the dynamics of the electrolyte for the system with and without gold become similar. As the potential increases, the Coulomb energy, similar for the Gr@Au and Gr systems, dominates the dynamics of the system. The van der Waals energy difference between the two systems becomes negligible and no significant differences remain.

## CONCLUSIONS

In order to investigate the influence of a gold substrate located below a single graphene layer on the electrical double layer structure and dynamics, we have compared a system with electrodes composed of nine Au(111) layers behind a layer of graphene with a system with electrodes composed only of a graphene layer. We focused on the pure ionic liquid [EMIM][TFSI] as electrolyte. The variation of the electronic density of state of graphene as a function of the applied potential, is taken into account by modulating the Gaussian width of the charge distribution of the carbon electrode atoms following the work carried out by Goloviznina et al.<sup>17</sup> In this way, we were able to vary the metallicity of the graphene and thus vary its electronic response to the adsorption of ions and to the applied potential. A significant effect of metallicity variation is observed in the capacitance profile.

The results of the molecular simulations show that the presence of gold modifies the profile of the charge distribution carried by the carbon atoms of the graphene layer. Despite its deep potential well, the gold is too far from the electrolyte to have a significant effect on the structure of the electrolyte at the interface with the electrode. This is a favorable outcome for experimentalists, as the presence of gold should not significantly affect the results obtained in spectroscopy studies, or when measuring the adsorbed mass using EQCM.

However, the presence of gold increases the strength of the interaction between the electrode and the electrolyte. In fact, the total interaction energy is higher in the presence of gold due to the increase in the van der Waals interaction term. Although we did not observe a major change in the structure of the electrolyte, this leads to a significant effect on the dynamics of the ions at low applied potentials. At low potentials, the

Coulomb energy is negligible compared to the van der Waals energy, so there is a major energy difference, of the order of 1000 kJ mol<sup>-1</sup>, between the two systems. For higher potentials, this difference becomes negligible due to the predominance of the Coulomb energy term. The dynamics of ion adsorption in the two systems therefore becomes similar as the potential increases above 1 V.

In the future, it could be interesting to better model the interaction between gold and graphene. Bringing gold and graphene into contact should lead to a depletion of charge from one material to the other, and this phenomenon depends on a number of parameters such as the distance between the two materials, the temperature, the facet of the gold substrate in contact with the graphene. This charge transfer leads to the creation of a dipole, generating a potential difference between the two materials. It could be interesting to apply different potentials to gold and graphene in order to observe the influence of this phenomenon on the electrode–electrolyte interfacial properties. In addition, graphene is flexible and can also have defects such as holes, steps and oxygen functions, which could have significant effects on the results obtained. Finally, graphene has both unusual and astonishing electronic properties that merit finer modeling on an electronic scale to take account of its versatility and all its nuances. A solution could be to resort to the use of data-driven approaches,<sup>44,45</sup> that allow to account explicitly for the electronic structure of the material at a reduced computational cost compared to the density functional theory calculations on which they are fitted. It would also be interesting to study several electrolytes. The performance of a supercapacitor is governed by the combination of electrode and electrolyte. Changing the electrolyte should alter the capacitance of the supercapacitor by affecting the size of the ions, which influences the composition of the adsorption layer, the electronic structure of the electrode and the distribution of atomic charges. In addition, the size of the ions and their interactions have an impact on their mobility and the charging dynamics of the system, while ion–electrode interactions shape the behavior of the ions at the interface.

## ASSOCIATED CONTENT

### Data Availability Statement

The data corresponding to the plots reported in this paper, as well as example input files for the MD simulations, are available in the Zenodo repository with the identifier 10.5281/zenodo.14720561.

### Supporting Information

The Supporting Information is available free of charge at <https://pubs.acs.org/doi/10.1021/acsnanoscienceau.4c00070>.

Radial charge–charge correlation function and atomic electrolyte densities at the interface with the electrodes at different applied potential differences (PDF)

## AUTHOR INFORMATION

### Corresponding Authors

Mathieu Salanne – *Physicochimie des Électrolytes et Nanosystèmes Interfaciaux, Sorbonne Université, CNRS, F-75005 Paris, France; Réseau sur le Stockage Electrochimique de l'Énergie (RS2E), Fédération de Recherche CNRS 3459, 80039 Amiens, France; [orcid.org/0000-0002-1753-491X](https://orcid.org/0000-0002-1753-491X); Email: [mathieu.salanne@sorbonne-universite.fr](mailto:mathieu.salanne@sorbonne-universite.fr)*



**Céline Merlet** – CIRIMAT, Université de Toulouse, CNRS, Université Toulouse 3 - Paul Sabatier, 31062 Toulouse Cedex 9, France; Réseau sur le Stockage Electrochimique de l'Énergie (RS2E), Fédération de Recherche CNRS 3459, 80039 Amiens, France; [orcid.org/0000-0003-3758-273X](https://orcid.org/0000-0003-3758-273X); Email: [celine.merlet@univ-tlse3.fr](mailto:celine.merlet@univ-tlse3.fr)

## Author

**Nicolas Gaudy** – CIRIMAT, Université de Toulouse, CNRS, Université Toulouse 3 - Paul Sabatier, 31062 Toulouse Cedex 9, France; Réseau sur le Stockage Electrochimique de l'Énergie (RS2E), Fédération de Recherche CNRS 3459, 80039 Amiens, France

Complete contact information is available at:

<https://pubs.acs.org/10.1021/acsnanoscienceau.4c00070>

## Author Contributions

CRedit: **Nicolas Gaudy** conceptualization, formal analysis, investigation, methodology, writing - original draft; **Mathieu Salanne** conceptualization, methodology, supervision, writing - review & editing; **Céline Merlet** conceptualization, methodology, resources, supervision, writing - review & editing.

## Notes

The authors declare no competing financial interest.

## ACKNOWLEDGMENTS

This project has received funding from the French National Research Agency (STORE-EX Labex project ANR-10LABX-76-01). This work was granted access to the HPC resources of TGCC under the allocations AD010911061R1 and A0110911061 made by GENCI.

## REFERENCES

- (1) Raccichimi, R.; Varzi, A.; Passerini, S.; Scrosati, B. The Role of Graphene for Electrochemical Energy Storage. *Nat. Mater.* **2015**, *15*, 271–279.
- (2) Levi, M. D.; Daikhin, L.; Aurbach, D.; Presser, V. Quartz Crystal Microbalance with Dissipation Monitoring (EQCM-D) for In-Situ Studies of Electrodes for Supercapacitors and Batteries: A Mini-Review. *Electrochem. Commun.* **2016**, *67*, 16–21.
- (3) Shpigel, N.; Levi, M. D.; Aurbach, D. EQCM-D Technique for Complex Mechanical Characterization of Energy Storage Electrodes: Background and Practical Guide. *Energy Storage Mater.* **2019**, *21*, 399–413.
- (4) Tsai, W.-Y.; Taberna, P.-L.; Simon, P. Electrochemical Quartz Crystal Microbalance (EQCM) Study of Ion Dynamics in Nanoporous Carbons. *J. Am. Chem. Soc.* **2014**, *136*, 8722–8728.
- (5) Wu, Y.-C.; Ye, J.; Jiang, G.; Ni, K.; Shu, N.; Taberna, P.-L.; Zhu, Y.; Simon, P. Electrochemical Characterization of Single Layer Graphene/Electrolyte Interface: Effect of Solvent on the Interfacial Capacitance. *Angew. Chem., Int. Ed.* **2021**, *60*, 13317–13322.
- (6) Ye, J.; Wu, Y.-C.; Xu, K.; Ni, K.; Shu, N.; Taberna, P.-L.; Zhu, Y.; Simon, P. Charge Storage Mechanisms of Single-Layer Graphene in Ionic Liquid. *J. Am. Chem. Soc.* **2019**, *141*, 16559–16563.
- (7) Lemaire, P.; Dargon, T.; Alves Dalla Corte, D.; Sel, O.; Perrot, H.; Tarascon, J.-M. Making Advanced Electrogravimetry as an Affordable Analytical Tool for Battery Interface Characterization. *Anal. Chem.* **2020**, *92*, 13803–13812.
- (8) Bendadesse, E.; Gervillière-Mouravieff, C.; Leau, C.; Goloviznina, K.; Rabuel, F.; Salanne, M.; Tarascon, J.-M.; Sel, O. Spotting Interface Structuring during Na-Insertion into the NaSICON Na<sub>3</sub>V<sub>2</sub>(PO<sub>4</sub>)<sub>3</sub> by EQCM and Operando Fiber Optic Infrared Spectroscopy. *Adv. Energy Mater.* **2023**, *13*, No. 2300930.
- (9) Ojaghlo, N.; Bratko, D.; Salanne, M.; Shafiei, M.; Luzar, A. Solvent–Solvent Correlations across Graphene: The Effect of Image Charges. *ACS Nano* **2020**, *14*, 7987–7998.
- (10) Mendez-Morales, T.; Burbano, M.; Haefele, M.; Rotenberg, B.; Salanne, M. Ion–Ion Correlations Across and Between Electrified Graphene Layers. *J. Chem. Phys.* **2018**, *148*, 193812.
- (11) Ntim, S.; Sulpizi, M. Role of Image Charges in Ionic Liquid Confined Between Metallic Interfaces. *Phys. Chem. Chem. Phys.* **2020**, *22*, 10786–10791.
- (12) Ntim, S.; Sulpizi, M. Effects of Shear Flow on the Structure and Dynamics of Ionic Liquids in a Metallic Nanoconfinement. *Phys. Chem. Chem. Phys.* **2021**, *23*, 24357–24364.
- (13) Heinz, H.; Vaia, R. A.; Farmer, B. L.; Naik, R. R. Accurate Simulation of Surfaces and Interfaces of Face-Centered Cubic Metals Using 12–6 and 9–6 Lennard-Jones Potentials. *J. Phys. Chem. C* **2008**, *112*, 17281–17290.
- (14) Wang, R.; Bi, S.; Presser, V.; Feng, G. Systematic Comparison of Force Fields for Molecular Dynamic Simulation of Au(111)/Ionic Liquid Interfaces. *Fluid Phase Equilib.* **2018**, *463*, 106–113.
- (15) Khomyakov, P. A.; Giovannetti, G.; Rusu, P. C.; Brocks, G.; van den Brink, J.; Kelly, P. J. First-Principles Study of the Interaction and Charge Transfer Between Graphene and Metals. *Physical review.* **2009**, *79*, No. 195425.
- (16) Pavlov, S.; Kozhevnikova, E.; Kislenco, S. Effect of the Number of Graphene Layers on the Electron Transfer Kinetics at Metal/Graphene Heterostructures. *J. Electroanal. Chem.* **2022**, *925*, No. 116895.
- (17) Goloviznina, K.; Fleischhaker, J.; Binninger, T.; Rotenberg, B.; Ers, H.; Ivanistsev, V.; Meissner, R.; Serva, A.; Salanne, M. Accounting for the Quantum Capacitance of Graphite in Constant Potential Molecular Dynamics Simulations. *Adv. Mater.* **2024**, *36*, No. 2405230.
- (18) Marin-Laflèche, A.; Haefele, M.; Scalfi, L.; Coretti, A.; Dufils, T.; Jeanmairet, G.; Reed, S. K.; Serva, A.; Berthin, R.; Bacon, C.; Bonella, S.; Rotenberg, B.; Madden, P. A.; Salanne, M. MetalWalls: A Classical Molecular Dynamics Software Dedicated to the Simulation of Electrochemical Systems. *J. Open Source Softw.* **2020**, *5*, 2373.
- (19) Coretti, A.; Bacon, C.; Berthin, R.; Serva, A.; Scalfi, L.; Chubak, I.; Goloviznina, K.; Haefele, M.; Marin-Laflèche, A.; Rotenberg, B.; Bonella, S.; Salanne, M. MetalWalls: Simulating Electrochemical Interfaces Between Polarizable Electrolytes and Metallic Electrodes. *J. Chem. Phys.* **2022**, *157*, 184801.
- (20) Reed, S. K.; Lanning, O. J.; Madden, P. A. Electrochemical Interface Between an Ionic Liquid and a Model Metallic Electrode. *J. Chem. Phys.* **2007**, *126*, No. 084704.
- (21) Siepmann, J. I.; Sprik, M. Influence of Surface Topology and Electrostatic Potential on Water/Electrode Systems. *J. Chem. Phys.* **1995**, *102*, 511–524.
- (22) Serva, A.; Scalfi, L.; Rotenberg, B.; Salanne, M. Effect of the Metallicity on the Capacitance of Gold–aqueous Sodium Chloride Interfaces. *J. Chem. Phys.* **2021**, *155*, No. 044703.
- (23) Canongia Lopes, J. N.; Deschamps, J.; Pádua, A. Modeling Ionic Liquids Using a Systematic All-Atom Force Field. *J. Phys. Chem. B* **2004**, *108*, 11250–11250.
- (24) Canongia Lopes, J. N.; Pádua, A. Molecular Force Field for Ionic Liquids Composed of Triflate or Bistriflylimide Anions. *J. Phys. Chem. B* **2004**, *108*, 16893–16898.
- (25) Bhargava, B. L.; Balasubramanian, S. Refined Potential Model for Atomistic Simulations of Ionic Liquid [bmim][PF<sub>6</sub>]. *J. Chem. Phys.* **2007**, *127*, 114510.
- (26) Chaban, V. Polarizability Versus Mobility: Atomistic Force Field for Ionic Liquids. *Phys. Chem. Chem. Phys.* **2011**, *13*, 16055–16062.
- (27) Zhang, Y.; Maginn, E. J. A Simple AIMD Approach to Derive Atomic Charges for Condensed Phase Simulation of Ionic Liquids. *J. Phys. Chem. B* **2012**, *116*, 10036–10048.
- (28) Schröder, C. Comparing Reduced Partial Charge Models with Polarizable Simulations of Ionic Liquids. *Phys. Chem. Chem. Phys.* **2012**, *14*, 3089–3102.



- (29) Sha, M.; Dou, Q.; Luo, F.; Zhu, G.; Wu, G. Molecular Insights into the Electric Double Layers of Ionic Liquids on Au(100) Electrodes. *ACS Appl. Mater. Interfaces* **2014**, *6*, 12556–12565.
- (30) Ferreira, E. S. C.; Pereira, C. M.; Cordeiro, M. N. D. S.; dos Santos, D. J. V. A. Molecular Dynamics Study of the Gold/Ionic Liquids Interface. *J. Phys. Chem. B* **2015**, *119*, 9883–9892.
- (31) Voroshyllova, I. V.; Ers, H.; Docampo-Álvarez, B.; Pikma, P.; Ivaništšev, V. B.; Cordeiro, M. N. D. Hysteresis in the MD Simulations of Differential Capacitance at the Ionic Liquid–Au Interface. *J. Phys. Chem. Lett.* **2020**, *11*, 10408–10413.
- (32) Martínez, L.; Andrade, R.; Birgin, E. G.; Martínez, J. M. PACKMOL: A Package for Building Initial Configurations for Molecular Dynamics Simulations. *J. Comput. Chem.* **2009**, *30*, 2157–2164.
- (33) Trenzado, J. L.; Rodríguez, Y.; Gutiérrez, A.; Cincotti, A.; Aparicio, S. Experimental and Molecular Modeling Study on the Binary Mixtures of [EMIM][BF<sub>4</sub>] and [EMIM][TFSI] Ionic Liquids. *J. Mol. Liq.* **2021**, *334*, No. 116049.
- (34) Pak, A. J.; Paek, E.; Hwang, G. S. Relative Contributions of Quantum and Double Layer Capacitance Toward the Supercapacitor Performance of Carbon Nanotubes in an Ionic Liquid. *Phys. Chem. Chem. Phys.* **2013**, *15*, 19741–19747.
- (35) Kornyshev, A. A. Double-Layer in Ionic Liquids: Paradigm Change? *J. Phys. Chem. B* **2007**, *111*, 5545–5557.
- (36) Bazant, M. Z.; Storey, B. D.; Kornyshev, A. A. Double Layer in Ionic Liquids: Overscreening versus Crowding. *Phys. Rev. Lett.* **2011**, *106*, No. 046102.
- (37) Yang, J.; Papaderakis, A. A.; Soo Roh, J.; Keerthi, A.; Adams, R. W.; Bissett, M. A.; Radha, B.; Dryfe, R. A. W. Measuring the Capacitance of Carbon in Ionic Liquids: From Graphite to Graphene. *J. Phys. Chem. C* **2024**, *128*, 3674–3684.
- (38) Merlet, C.; Rotenberg, B.; Madden, P. A.; Salanne, M. Computer simulations of ionic liquids at electrochemical interfaces. *Phys. Chem. Chem. Phys.* **2013**, *15*, 15781–15792.
- (39) Merlet, C. Modélisation de l'Adsorption des Ions dans les Carbones Nanoporeux; Theses; Université Pierre et Marie Curie - Paris VI, 2013.
- (40) Merlet, C.; Salanne, M.; Rotenberg, B.; Madden, P. A. Influence of Solvation on the Structural and Capacitive Properties of Electrical Double Layer Capacitors. *Electrochim. Acta* **2013**, *101*, 262–271.
- (41) Elliott, J. D.; Troisi, A.; Carbone, P. A. QM/MD Coupling Method to Model the Ion-Induced Polarization of Graphene. *J. Chem. Theory. Comput.* **2020**, *16*, 5253–5263.
- (42) Scalfi, L.; Rotenberg, B. Microscopic Origin of the Effect of Substrate Metallicity on Interfacial Free energies. *Proc. Natl. Acad. Sci. U. S. A.* **2021**, *118*, No. e2108769118.
- (43) Wirth-Lima, A. J.; Bezerra-Fraga, W. Graphene-Based BPSK and QPSK Modulators Working at a Very High Bit Rate (up Tb/s range). *Opt. Quantum Electron.* **2021**, *53*, 271.
- (44) Grisafi, A.; Bussy, A.; Salanne, M.; Vuilleumier, R. Predicting the Charge Density Response in Metal Electrodes. *Phys. Rev. Mater.* **2023**, *7*, No. 125403.
- (45) Grisafi, A.; Salanne, M. Accelerating QM/MM Simulations of Electrochemical Interfaces Through Machine Learning of Electronic Charge Densities. *J. Chem. Phys.* **2024**, *161*, No. 024109.